ARTICLE IN PRESS

Optics Communications xxx (xxxx) xxx–xxx

Contents lists available at ScienceDirect

Optics Communications

journal homepage: www.elsevier.com/locate/optcom

Multiframe super resolution reconstruction method based on light field angular images

Shubo Zhou, Yan Yuan*, Lijuan Su, Xiaomin Ding, Jichao Wang

Beihang University, Key Laboratory of Precision Opto-mechatronics Technology of Ministry of Education, Xueyuan Road No. 37, Haidian District, Beijing 100191, China

ARTICLE INFO

Keywords:
Plenoptic imaging
Observation model
Super resolution
Angular image

ABSTRACT

The plenoptic camera can directly obtain 4-dimensional light field information from a 2-dimensional sensor. However, based on the sampling theorem, the spatial resolution is greatly limited by the microlenses. In this paper, we present a method of reconstructing high-resolution images from the angular images. First, the ray tracing method is used to model the telecentric-based light field imaging process. Then, we analyze the subpixel shifts between the angular images extracted from the defocused light field data and the blur in the angular images. According to the analysis above, we construct the observation model from the ideal high-resolution image to the angular images. Applying the regularized super resolution method, we can obtain the super resolution result with a magnification ratio of 8. The results demonstrate the effectiveness of the proposed observation model.

1. Introduction

The plenoptic camera can directly obtain 4-dimensional light field information from a 2-dimensional sensor [1,2]. However, the spatial resolution is greatly limited by the microlenses because the sensor is subdivided into various sub-regions in the imaging process. To enhance the spatial resolution of the light field image, researchers apply image processing technology such as the super resolution (SR) method to reconstruct a high-resolution (HR) image from low-resolution (LR) data [3].

We classify the light field SR approaches into two categories: subimage-based SR methods and angular image-based SR methods. The subimage is formed by extracting pixels under a microlens. The angular image is formed by extracting the same pixels under each microlens [4].

The subimage-based SR methods reconstruct the HR image by image restoration. Bishop et al. use geometric optics theory to calculate the blur size generated by the main lens and microlens, then apply the defocus blur model to define the light field point spread function (PSF), which varies by depth. Finally, they propose a Bayesian theory-based method to reconstruct the HR image [3,4]. Similar approaches can also be found in the literature [5,6]. Cho D et al. [5] propose a learning based interpolation method which can obtain a higher quality image. K. Mitra and A. Veeraraghavan [6] model the light field sub-images by using a Gaussian mixture model. Based on the model, they design a prior and spatially super resolve the light field data by a factor of 4. Recently, the scalar diffraction theory has been applied in light field analysis. In the case of monochromatic illumination, Shroff et al. acquire the plenoptic camera PSF using Fresnel diffraction theory, and then a deconvolution-like method is proposed to reconstruct the HR image [7]. Other similar approaches can also be found in the literature [8–10].

The angular image-based SR methods reconstruct the HR image by multiframe super resolution methods. Zhou Z et al. analyze the sub-pixel shift between angular images extracted from the defocused light field data, and then apply the Maximum a Posterior (MAP) SR method to reconstruct the HR image [11]. Another similar approach can also be found in the literature [12]. Xu Z et al. construct an observation model between the ideal scene and the angular images and use it to super resolve the HR image. However, the observation matrix is not analytically obtained.

In this paper, we model the telecentric-based light field imaging process, and then construct an observation model between the ideal HR image and the angular images. In the observation model, the observation matrix can be analytically obtained. With the observation model, a regularized super resolution method is applied to reconstruct the HR image. The remainder of this paper is organized as follows. Section 2 introduces the observation model and the regularized SR method, Section 3 shows the SR results of the light-field data synthesis, Section 4 shows the SR results of real light-field data, and Section 5 is the conclusion.

* Corresponding author.
E-mail address: yuanyan@buaa.edu.cn (Y. Yuan).

http://dx.doi.org/10.1016/j.optcom.2017.03.019
Received 12 December 2016; Received in revised form 25 February 2017; Accepted 6 March 2017

Please cite this article as: Shubo, Z., Optics Communications (2017), http://dx.doi.org/10.1016/j.optcom.2017.03.019

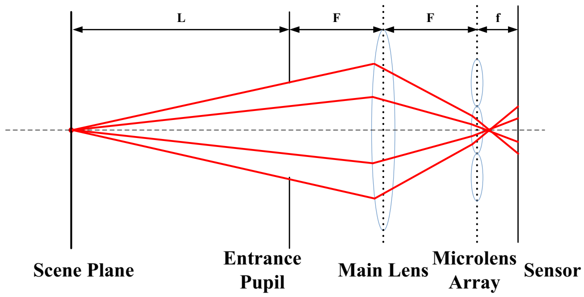

Fig. 1. Schematic illustration of telecentric-based plenoptic camera. The size of the microlenses is exaggerated to make the optical path more clearly.

2. The observation model

The schematic illustration of a telecentric based plenoptic camera is shown in Fig. 1. In the case of finite object distance, the light field data is strictly defocused, as the microlens array is positioned on the back focal plane of the main lens. Meanwhile, in a telecentric-based plenoptic camera, the center of a subimage is consistent with the center of the relevant microlens, which can reduce the complexity of plenoptic camera calibration.

Based on Fig. 1, we define all the parameters in Table 1, including the plenoptic camera parameters and the imaging parameters.

First, we assume that the energy transfer efficiency is identical when the angular rays pass though the plenoptic camera. The origin of the optical system is in the center of the entrance pupil. Supposing the number of angular rays emitted from p is nxn, we can define the angular ray by calculating the distance between the ray and the center of the entrance pupil using Eq. (1).

$$\begin{bmatrix}\Delta x\\ \Delta y\end{bmatrix}=\begin{bmatrix}\frac{(k-1)D}{(n-1)}-\frac{D}{2}\\ \frac{(j-1)D}{(n-1)}-\frac{D}{2}\end{bmatrix}=\begin{bmatrix}\frac{(2k-n-1)D}{2(n-1)}\\ \frac{(2j-n-1)D}{2(n-1)}\end{bmatrix}1\le k\le n,\ 1\le j\le n \tag{1}$$

k and j mean the index of the angular ray. When k and j are equal to $\frac{n+1}{2}$, the angular ray is the principle ray. Based on Fig. 1, rays passing through the entrance pupil are diffused by microlenses array. Therefore, the sub aperture can be defined by dividing the entrance pupil, while each pixel on the sensor collects the rays passing through an identical sub aperture. In this paper, we use 3x3 rays to describe a sub aperture. Fig. 2 shows a 2D section, while the red rays are the center rays, and the blue rays are the bound rays.

The sub aperture's diameter is $\frac{D\mu}{d}$. Assuming $\frac{d}{\mu}$ is an integer, n can be calculated by Eq. (2):

$$n=\frac{2d}{\mu}+1 \tag{2}$$

Table 1
Plenoptic camera parameters and imaging parameters.

Camera parameters	
Entrance pupil diameter	D
Microlens diameter	d
Main lens focal length	F
Microlens focal length	f
Microlens center	$c=[c_x, c_y]$
Size of a sensor pixel	μ
Number of microlenses	MxN
Imaging parameters	
Scene point	$p=[x, y, z]$
Focused position of p passing through the main lens	$p'=[x', y', z']$
Projection of p onto the microlens	$p_b=[p_{bx}, p_{by}]$
Projection of p onto the sensor	$p''=[x'', y'', z'']$
Object distance	L
Defocus amount	z

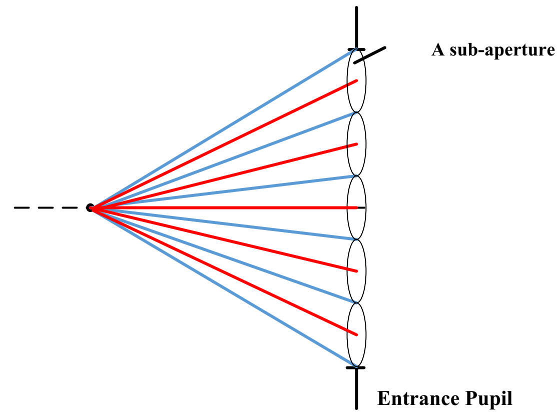

Fig. 2. Schematic figure of the sub aperture and the angular rays.

For one sub-aperture, 3 types of the angular rays can be defined by Eqs. (3)–(5). Eq. (3) is the upper bound ray, Eq. (4) is the center ray, and Eq. (5) is the lower bound ray.

$$\begin{bmatrix}\Delta x_u\\ \Delta y_u\end{bmatrix}=\begin{bmatrix}\frac{[(k_1+1)\mu-d]D}{2d}\\ \frac{[(j_1+1)\mu-d]D}{2d}\end{bmatrix} \tag{3}$$

$$\begin{bmatrix}\Delta x_c\\ \Delta y_c\end{bmatrix}=\begin{bmatrix}\frac{(k_1\mu-d)D}{2d}\\ \frac{(j_1\mu-d)D}{2d}\end{bmatrix} \tag{4}$$

$$\begin{bmatrix}\Delta x_l\\ \Delta y_l\end{bmatrix}=\begin{bmatrix}\frac{[(k_1-1)\mu-d]D}{2d}\\ \frac{[(j_1-1)\mu-d]D}{2d}\end{bmatrix} \tag{5}$$

where k_1, j_1 are even, ranging from 2 to $\frac{2d}{\mu}$.

Using the Gaussian formula, p' can be calculated by Eq. (6):

$$p'=\begin{bmatrix}x'\\ y'\\ z'\end{bmatrix}=\begin{bmatrix}-\frac{Fx}{L}\\ -\frac{Fy}{L}\\ 2F+\frac{F^2}{L}\end{bmatrix} \tag{6}$$

Therefore, using similar triangles, p_b can be obtained by Eq. (7):

$$p_b=\begin{bmatrix}p_{bx}\\ p_{by}\end{bmatrix}=\begin{bmatrix}x'-\frac{z\Delta x}{F}\\ y'-\frac{z\Delta y}{F}\end{bmatrix} \tag{7}$$

Suppose M and N are odd. From Eq. (7), we can find the position where the microlens intersects with the angular ray, and the center of the microlens can be obtained by Eq. (8):

$$c=\begin{bmatrix}c_x\\ c_y\end{bmatrix}=\begin{bmatrix}\lfloor\frac{x_{bx}}{d}+\frac{1}{2}\rfloor\bullet d\\ \lfloor\frac{x_{by}}{d}+\frac{1}{2}\rfloor\bullet d\end{bmatrix} \tag{8}$$

where $\lfloor x\rfloor$ is an integralized function that rounds to the nearest integer less than or equal to x. Using similar triangles, the projection of p onto the sensor can be obtained as Eq. (9):

$$p''=\begin{bmatrix}x''\\ y''\\ z''\end{bmatrix}=\begin{bmatrix}c_x-\frac{f\Delta x}{F}\\ c_y-\frac{f\Delta y}{F}\\ 2F+f\end{bmatrix} \tag{9}$$

According to the analysis above, we find that the identical angular information is imaged on the identical position behind each microlens. Therefore, when the light field data are focused, the pixels under a microlens consist of the same scene information. On the other hand, when the light field data is defocused, p_b is not identical, and the